Sha *et al.*
EURASIP Journal on Advances in Signal Processing (2022) 2022:25
https://doi.org/10.1186/s13634-022-00859-2

EURASIP Journal on Advances in Signal Processing

RESEARCH Open Access

A low complexity STPAP algorithm based on an alternating polarization-sensitive array

Shuang Sha[1], Tingting Lyu[1*], Hao Zhang[1,2], T. Aaron Gulliver[2] and Ying Dong[1]

*Correspondence:
tingtinglu@ouc.edu.cn
[1] China Open Studio for Marine High Frequency Communications, Pilot National Laboratory for Marine Science and Technology (Qingdao), Institution of Information Science and Engineering, Ocean University of China, Qingdao 266100, China
Full list of author information is available at the end of the article

Abstract

Background: Space–time adaptive processing (STAP) has been widely used in the fields of communication, radar, and navigation anti-jamming. However, the traditional scalar arrays used with STAP have limitations because they can only obtain spatial information. To improve the performance, joint space–time filtering is proposed using an alternating polarization-sensitive array (APSA). Compared to a dual-polarization sensitive array (DPSA), this array can provide polarization information and reduce the computational complexity.

Methods: An alternating polarization-sensitive array space–time polarization adaptive processing (APSA-STPAP) algorithm is proposed based on the linear constraint minimum variance (LCMV) criterion. Different from the traditional LCMV criterion, the space–time polarization joint steering vector of the desired and interference signals is used as the constraint matrix, and the "set 1" and "set 0" conditions are used as the constraint conditions to effectively suppress the interference signals and enhance the desired signals.

Results: Simulation results are presented which show the following. (1) Filtering with the proposed APSA-STPAP algorithm is similar to that with the DPSA-STPAP algorithm. From the perspective of the spatial, time, and polarization domains, it can form nulls in the directions of the interference and realize space–time-polarization adaptive processing. (2) The APSA-STPAP algorithm has lower computational complexity than the DPSA-STPAP algorithm. Moreover, the dipole of the alternating polarization sensitive array is halved, which reduces the coupling effect between electric dipoles and makes implementation easier. (3) The APSA-STPAP algorithm maintains good anti-interference performance even when the electric dipole and anti-jamming degrees of freedom are reduced by half, and the anti-jamming performance is similar to that of a polarization-sensitive array. There is little difference between the anti-interference performance of the APSA-STPAP and DPSA-STPAP algorithms when SNR ≥ -10 dB.

Keywords: Alternating polarization-sensitive array, Polarization-sensitive array, Space–time-polarization adaptive processing, LCMV

1 Introduction

Antenna array processing with spatial filtering has been shown to be effective in canceling interference in received signals such as in the global navigation satellite system (GNSS) and radar systems [1]. This approach employs weights on the signals received by the

array elements to form nulls in the directions of the interference while steering the array response toward the desired signals. These weights can be changed adaptively [2]. Space–time adaptive processing (STAP) is based on spatial filtering [3]. In STAP, each array element is followed by a time domain finite impulse response (FIR) filter. STAP has been used to adaptively process radar signals using both space and time sampling [4, 5]. This solves the problem of ground clutter suppression in radar signals. STAP has also been applied for anti-interference in GNSS [6, 7]. An adaptive antenna array was employed for interference reduction which increases the number of degrees of freedom for signal processing. However, if the interference directions are close to those of the desired signals, STAP will degrade the desired signals when nulling the interference. Thus, polarization domain information is utilized to distinguish and suppress the interference.

In [7–12], space-polarization adaptive processing (SPAP) was introduced to suppress interference in the joint space-polarization domain. Further, STPAP was proposed in [13] to mitigate interference. The polarization information of a signal can be obtained using a dual-polarization sensitive array (DPSA). Compared with traditional antenna arrays, DPSA has several advantages such as strong interference suppression, robust detection, high resolution, and polarization multiple access [14, 15]. Consequently, DPSA has been widely employed in radar, remote sensing, seismic signal processing, and wireless communication systems [16]. However, the complex structure and resulting implementation difficulties limit the use of polarization-sensitive arrays. Thus, the alternating polarization sensitive array (APSA) was proposed [17]. A DPSA is composed of electric dipoles along the x and y axes which can receive electric field information from the x and y directions [17–19]. The APSA structure has half the complexity of DPSA, but the polarization information is also reduced by half. However, APSA and DPSA have similar filtering performance [19].

In this paper, space–time-polarization adaptive processing is employed with APSA, and an alternating polarization-sensitive array space–time polarization adaptive processing (APSA-STPAP) algorithm based on the linear constraint minimum variance (LCMV) criterion is proposed. The joint steering loss of the desired and interference signals in the spatial, time, and polarization domains is used as the constraint matrix, and the "set 1" and "set 0" conditions are taken as the constraint conditions to effectively suppress the interference signals and enhance the desired signals.

The remainder of this paper is organized as follows: Section 2 presents the polarization model, APSA structure, and signal model. The proposed APSA-STPAP filtering algorithm based on the LCMV criterion is given in Sect. 3. Simulation results are presented in Sect. 4 to evaluate the performance and effectiveness of the proposed algorithm. Moreover, the proposed APSA-STPAP algorithm is compared with the DPSA-STPAP algorithm. Finally, Sect. 5 concludes the paper.

2 Alternating polarization-sensitive array and the received signal model

2.1 Polarization model

Figure 1 illustrates a transverse electric (TE) wave incident from direction (θ, φ) with respect to the reference point O, where $\theta \in [-90°, 90°]$ is the pitch angle and $\varphi \in [0°, 360°]$ is the azimuth angle [20]. The pitch angle refers to the acute angle between the direction

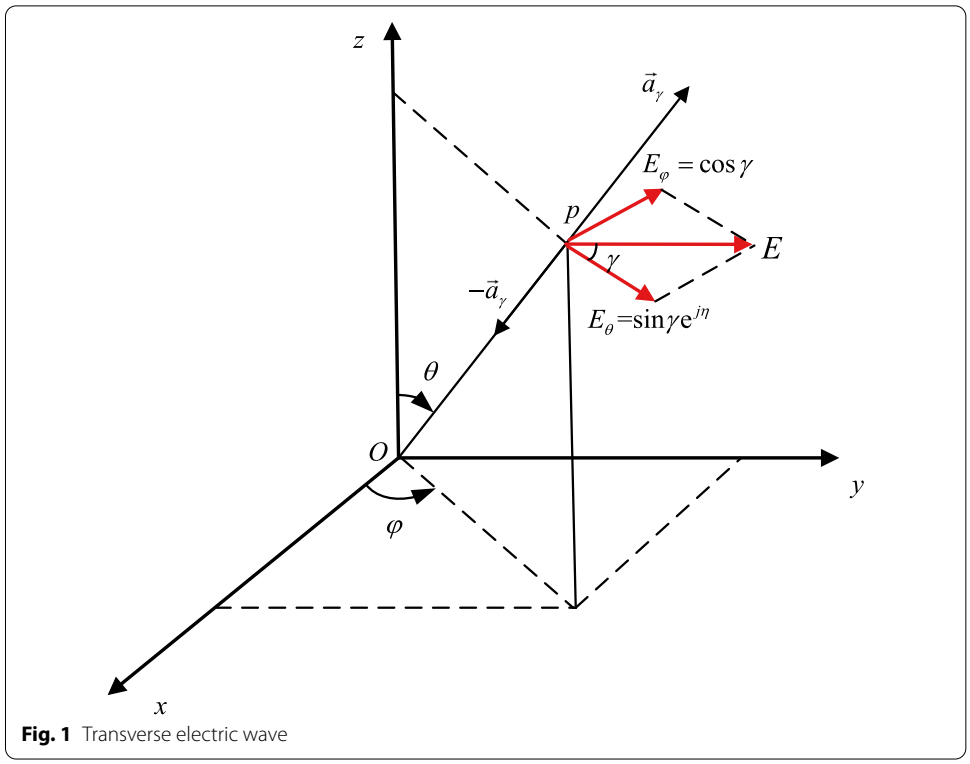

Fig. 1 Transverse electric wave

of the incoming signal and the normal of the antenna. The azimuth angle refers to the angle between the projection of the incoming signal on the antenna and the reference direction. Denote the transient electric field vector at point P as $\vec{\mathbf{E}}$. This can be written as $\vec{\mathbf{E}} = E_\theta \vec{\mathbf{e}}_\theta + E_\varphi \vec{\mathbf{e}}_\varphi$ where $(\vec{\mathbf{e}}_\theta, \vec{\mathbf{e}}_\varphi)$ is a pair of orthonormal vector and E_θ and E_φ denote the transient projections in the $\vec{\mathbf{e}}_\theta$ and $\vec{\mathbf{e}}_\varphi$ directions, respectively. The magnitudes of the electric field components are $E_\theta = \sin\gamma e^{j\eta}$ and $E_\varphi = \cos\gamma$ where (γ, η) are the polarization parameters which describe the polarization mode of the TE wave. $\gamma \in [0°, 90°]$ is the amplitude ratio between the horizontal and vertical components of the electric field and $\eta \in [-180°, 180°]$ is the phase difference between the horizontal and vertical components of the electric field. According to the orientation of the endpoint of the transient electric field vector, the TE wave can be classified as linear polarization, circular polarization, or elliptical polarization (EP) [21]. Moreover, linear polarization can be classified as horizontal polarization (HP) or vertical polarization (VP). Circular polarization can be classified as right-hand circular polarization (RHCP) or left-hand circular polarization (LHCP). These modes can be defined by the polarization parameters given in Table 1. The polarization vector of the received signal at the array can be expressed as [22, 23]

$$\mathbf{s}_p = \begin{bmatrix} E_x \\ E_y \\ E_z \\ H_x \\ H_y \\ H_z \end{bmatrix} = \begin{bmatrix} -\sin\varphi & \cos\theta\cos\varphi \\ \cos\varphi & \cos\theta\sin\varphi \\ 0 & -\sin\theta \\ \cos\theta\cos\varphi & \sin\varphi \\ \cos\theta\sin\varphi & -\cos\varphi \\ -\sin\theta & 0 \end{bmatrix} \begin{bmatrix} \cos\gamma \\ \sin\gamma e^{j\eta} \end{bmatrix} \tag{1}$$

Table 1 The parameters for different polarization modes

Polarization mode	Amplitude ratio (γ)	Phase difference (η)
HP	0	− 180, 0, 180
VP	90	− 180, 0, 180
RHCP	45	− 90
LHCP	45	90
EP	[0, 90]	[− 180, 180]

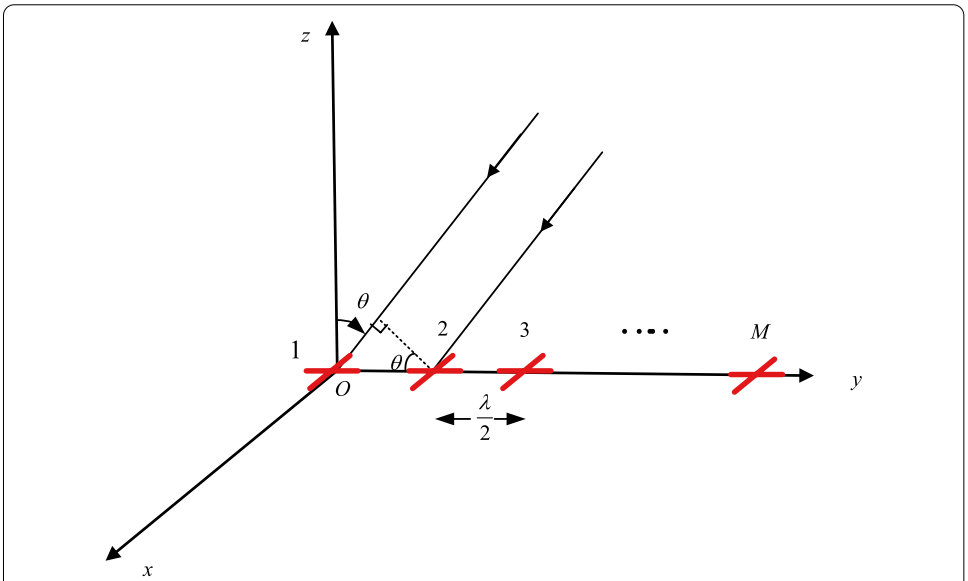

Fig. 2 Dual-polarized ULA array

2.2 Iternating polarization-sensitive array structure

An APSA contains M dual-polarized elements as shown in Fig. 2. The polarization information is obtained via correlation of the x and y channels, and the spatial information is obtained from the phase lag. For simplicity and without loss of generality a uniform linear array (ULA) along the y-axis is considered here, and the azimuth angle is 90°, i.e., $\varphi = 90°$.The distance between two elements, d, is assumed to be half the wavelength of the desired signals $d = \lambda/2$.

The APSA used here is based on a PSA and is shown in Fig. 3 [17–19]. Compared to an APSA, each array element is along the x-axis or y-axis of the dipole alternately.

Figure 4 illustrates the structure of the proposed alternating polarization-sensitive array polarization space–time adaptive processing (APSA-STPAP) algorithm. This is similar to a conventional STAP with the LCMV criterion algorithm which has one RF chain for each antenna element [24]. However, the APSA-STPAP algorithm has RF chains for the vertical or horizontal dipole components. After the RF

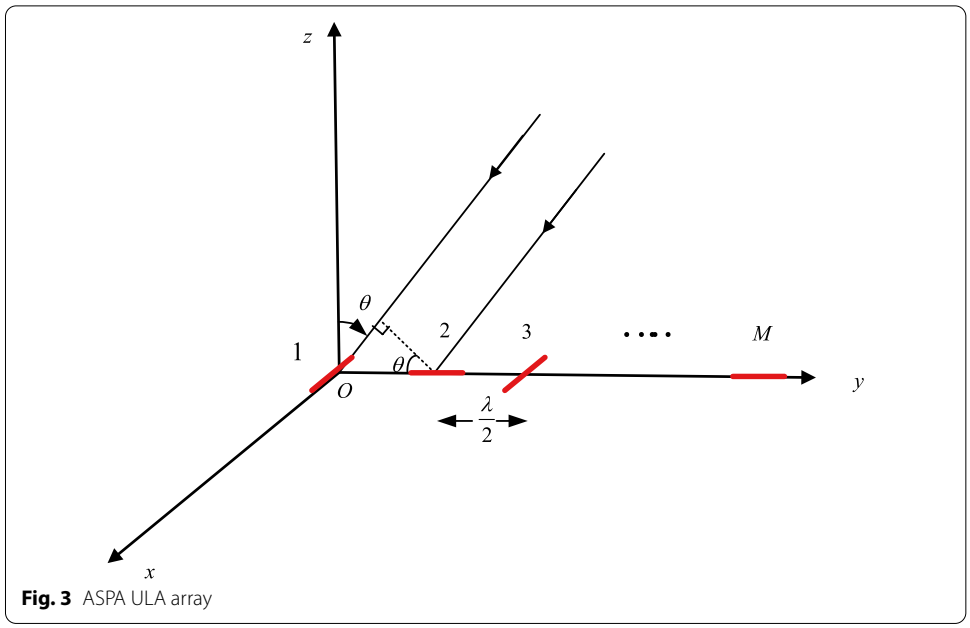

Fig. 3 ASPA ULA array

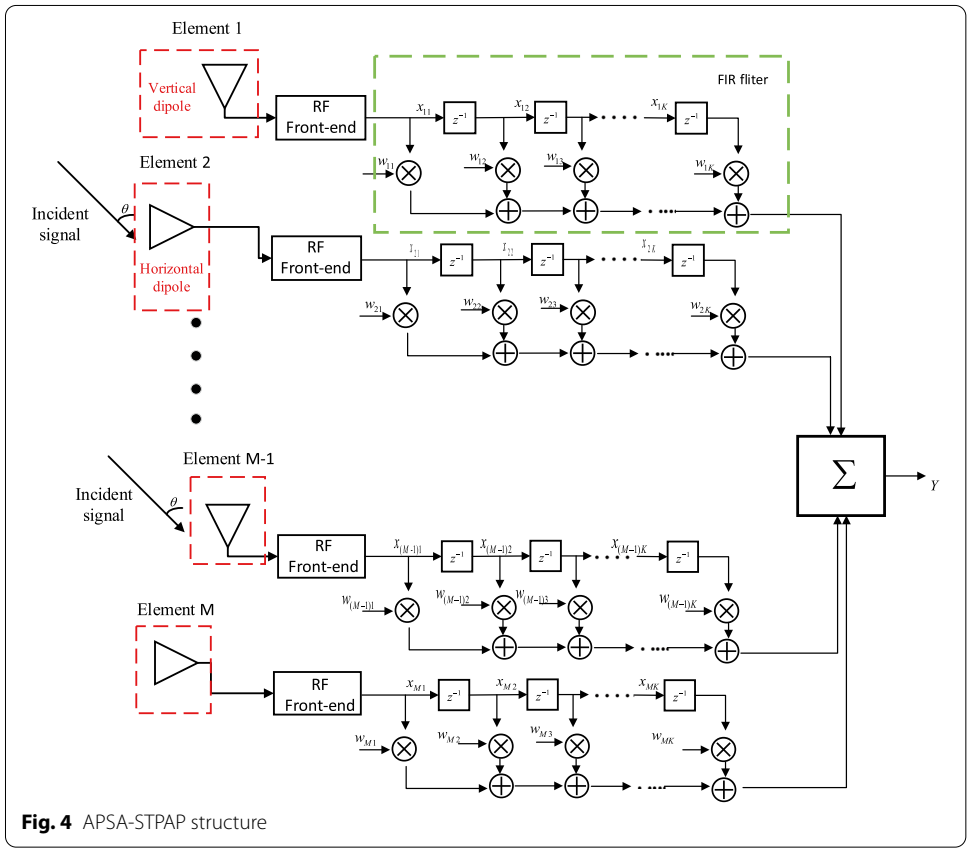

Fig. 4 APSA-STPAP structure

front end, signals from each antenna component pass through an FIR filter with K taps.

2.3 Array steering vector

The joint space–time polarization steering vector for a dual-polarized ULA can be expressed as

$$\mathbf{s}_{\mathrm{STP}}(\theta,f,\gamma,\eta) = \mathbf{s}_S(\theta) \otimes \mathbf{s}_P(\gamma,\eta) \otimes \mathbf{s}_T(f) \tag{2}$$

where $\otimes$ denotes the Kronecker product. The length M space steering vector is

$$\begin{aligned}\mathbf{s}_S(\theta) &= \left[1\ q^1\ q^2 \cdots q^{M-1}\right]^T \\ &= \left[1\ \exp(-j2\pi\frac{d}{\lambda}\sin\theta)\cdots\exp(-j2\pi(M-1)\frac{d}{\lambda}\sin\theta)\right]^T\end{aligned} \tag{3}$$

where $q = e^{-j2\pi\frac{d}{\lambda}\sin\theta}$ is the spatial phase factor and $(\cdot)^T$ denotes transpose. The length K time domain steering vector can be expressed as

$$\mathbf{s}_T(f) = [1 \quad \exp(-j2\pi f T_s) \quad \cdots \quad \exp(-j2\pi(K-1)fT_s)]^T \tag{4}$$

where f is the intermediate frequency after the signal passes through the RF front end and T_s is the sampling period of the FIR filter.

From (1), The polarization domain steering vector for a dual-polarized ULA can be written as

$$\mathbf{s}_P(\theta,\gamma,\eta) = \begin{bmatrix}-1 & 0\\ 0 & \cos\theta\end{bmatrix}\begin{bmatrix}\cos\gamma\\ \sin\gamma e^{j\eta}\end{bmatrix} = \begin{bmatrix}-\cos\gamma\\ \cos\theta\sin\gamma e^{j\eta}\end{bmatrix} \tag{5}$$

Similar to (2), the joint polarization space–time steering vector for an alternating polarization-sensitive array STPAP is given by

$$\mathbf{s}_{\mathrm{ASTP}}(\theta,f,\gamma,\eta) = \mathbf{s}_{\mathrm{AS}}(\theta) \otimes \mathbf{s}_{\mathrm{AP}}(\gamma,\eta) \otimes \mathbf{s}_T(f) \tag{6}$$

The length $\frac{M}{2}$ APSA space steering vector can be written as

$$\begin{aligned}\mathbf{s}_S(\theta) &= \left[1q^2q^4\cdots q^{M-2}\right]^T \\ &= \left[1\ \exp(-j4\pi\frac{d}{\lambda}\sin\theta)\cdots\exp(-j2\pi(M-2)\frac{d}{\lambda}\sin\theta)\right]^T\end{aligned} \tag{7}$$

The distance between adjacent dipoles in each direction is assumed to be the desired signal wavelength. The polarization domain steering vector for an APSA can be expressed as

$$\begin{aligned}\mathbf{s}_P(\theta,\gamma,\eta) &= \begin{bmatrix} -1 & 0 \\ 0 & \cos\theta \end{bmatrix} \begin{bmatrix} \cos\gamma \\ q\sin\gamma e^{j\eta} \end{bmatrix} \\ &= \begin{bmatrix} -\cos\gamma \\ \cos\theta\sin\gamma e^{j(\eta+2\pi\frac{d}{\lambda}\sin\theta)} \end{bmatrix}\end{aligned} \tag{8}$$

Comparing (2) and (6), the dimension of the APSA joint steering vector is half that of the DPSA. This reduces the number of calculations and thus the computational complexity.

2.4 Array signal receiving model

The nth, $1 \le n \le L$, signal block received by the array is given by

$$\mathbf{X}(n) = \mathbf{A}\mathbf{s}(n) + \mathbf{J}(n) + \mathbf{V}(n) \tag{9}$$

where $\mathbf{A}$ is the joint vector matrix, $\mathbf{s}(n)$ is the amplitude vector of the desired signal, $\mathbf{J}(n)$ is the interference signal matrix, and $\mathbf{V}(n)$ is a white Gaussian noise vector with elements having mean 0 and variance σ^2. We then have

$$\mathbf{X} = [\mathbf{x}_{11}(n), \cdots, \mathbf{x}_{1K}(n), \cdots, \mathbf{x}_{M1}(n), \cdots, \mathbf{x}_{MK}(n)]^T \tag{10}$$

Assume the pth, $p = 1, 2, \ldots, P$, desired signal has intermediate frequency f_p, incident angle θ_p, and polarization parameters (γ_p, η_p), and the qth, $q = 1, 2, \cdots, Q$, interference signal has intermediate frequency f_q, incident angle θ_q, and polarization parameters (γ_q, η_q). Then from Fig. 4, the received signal model for the nth block can be written as

$$\begin{aligned}\mathbf{x}_{\mathrm{ASTP}}(n) = &\sum_{p=1}^{P} \mathbf{s}_{\mathrm{ASTP}}(\theta_p, f_p, \gamma_p, \eta_p)\mathbf{s}_p(n) \\ &+ \sum_{q=1}^{Q} \mathbf{s}_{\mathrm{ASTP}}(\theta_q, f_q, \gamma_q, \eta_q)\mathbf{j}_q(n) + \mathbf{v}_{\mathrm{ASTP}}(n)\end{aligned} \tag{11}$$

3 APSA-STPAP algorithm based on LCMV

Assuming that the direction of arrival (DOA) and polarization information of the desired signal is known, the LCMV criterion can be employed in the APSA-STPAP algorithm. The array output can then be expressed as [25]

$$\mathbf{y}(n) = \mathbf{w}^H \mathbf{x}_{ASTP}(n) \tag{12}$$

where w is a length $M \times K$ weight vector and $(\cdot)^H$ denotes Hermitian. This vector can be written as

$$\mathbf{w} = [w_{11}, \ldots, w_{1K}, \ldots, w_{M1}, \ldots, w_{MK}] \tag{13}$$

The output signal power is

$$\begin{aligned}\mathbf{P} &= E\left[\left|\mathbf{y}(n)\right|^2\right] \\ &= E\left[\mathbf{w}^H\mathbf{x}_{\mathrm{ASTP}}(n)\mathbf{x}_{\mathrm{ASTP}}^H(n)\mathbf{w}\right] \\ &= \mathbf{w}^H\mathbf{R}\mathbf{w}\end{aligned} \tag{14}$$

where $\mathbf{R} = E[\mathbf{x}_{\mathrm{ASTP}}(n)\mathbf{x}_{\mathrm{ASTP}}^H(n)]$ is the covariance matrix of the received signals and $E[\cdot]$ denotes expectation. This matrix is unknown but a sampled covariance matrix [14] can be obtained as

$$\hat{\mathbf{R}} = \frac{1}{L}\sum_{n=1}^{L}[\mathbf{x}_{\mathrm{ASTP}}(n)\mathbf{x}_{\mathrm{ASTP}}^H(n)] \tag{15}$$

where L is the number of samples.

The constraint conditions of the weight vector to recover the desired signals from θ_p and suppress the interference from θ_q can be expressed as

$$\begin{cases}\mathbf{w}^H\mathbf{s}_{\mathrm{ASTP}}(\theta_p, f_p, \gamma_p, \eta_p) = 1 \\ \mathbf{w}^H\mathbf{s}_{\mathrm{ASTP}}(\theta_q, f_q, \gamma_q, \eta_q) = 0\end{cases} \tag{16}$$

The constraint condition in the direction of the desired signals is "set to 1," and the constraint condition in the direction of the interference signals is "set to 0." This is because the direction of the array receive beam pattern is expected to be toward the desired signals and the zero point is expected to point to the interference signals.

To ensure signal reception in the directions of the P desired signals and the null to suppress interference in the direction of the Q interfering signals, the constraints on the weight vector can be expressed as

$$\mathbf{C}^H\mathbf{w} = \mathbf{f} \tag{17}$$

where $\mathbf{C}$ is an $MK \times (P+Q)$ constraint matrix and $\mathbf{f}$ is the response vector. These can be written as

$$\begin{aligned}&\mathbf{C} = [\mathbf{s}_{\mathrm{ASTP}}(\theta_1, f_1, \gamma_1, \eta_1), \ldots, \mathbf{s}_{\mathrm{ASTP}}(\theta_P, f_P, \gamma_P, \eta_P), \\ &\mathbf{s}_{\mathrm{ASTP}}(\theta_{P+1}, f_{P+1}, \gamma_{P+1}, \eta_{p+1}), \ldots, \mathbf{s}_{\mathrm{ASTP}}(\theta_{P+Q}, f_{P+Q}, \gamma_{P+Q}, \eta_{p+Q})]\end{aligned} \tag{18}$$

$$\mathbf{f} = \underbrace{[1, \ldots, 1}_{P}, \underbrace{0, \ldots, 0]^T}_{Q} \tag{19}$$

The optimization problem can then be expressed as

$$\begin{cases}\min \quad \mathbf{w}^H\hat{\mathbf{R}}\mathbf{w} \\ \text{s.t.} \quad \mathbf{C}^H\mathbf{w} = \mathbf{f}\end{cases} \tag{20}$$

Using Lagrange multipliers, the optimal LCMV weight vector is [25]

$$\mathbf{w} = \hat{\mathbf{R}}^{-1}\mathbf{C}(\mathbf{C}^H\hat{\mathbf{R}}^{-1}\mathbf{C})^{-1}\mathbf{f} \tag{21}$$

The resulting array pattern is

$$\mathbf{F}(\theta,\varphi,f,\gamma,\eta)=\mathbf{w}^H\mathbf{s}_{\mathrm{ASTP}}(\theta,f,\gamma,\eta) \tag{22}$$

and the corresponding normalized array pattern is

$$\mathbf{G}(\theta,\varphi,f,\gamma,\eta) = 20\log_{10}\frac{\left|\mathbf{F}(\theta,\varphi,f,\gamma,\eta)\right|}{\left|\mathbf{F}(\theta,\varphi,f,\gamma,\eta)\right|_{\max}} \tag{23}$$

The signal covariance matrix $\mathbf{R}_s$ and the interference plus noise covariance matrix $\mathbf{R}_{j+\nu}$ are

$$\mathbf{R}_s = E\left[\mathbf{x}_s(n)\mathbf{x}_s^H(n)\right] \tag{24}$$

$$\mathbf{R}_{j+\nu} = E\left[\mathbf{x}_{j+\nu}(n)\mathbf{x}_{j+\nu}^H(n)\right] \tag{25}$$

Then the output signal power after beamforming can be written as

$$\begin{aligned}\mathbf{P}_s &= E\left[\left|\mathbf{y}_s(n)\right|^2\right]\\ &= E\left[\mathbf{w}^H\mathbf{x}_s(n)\mathbf{x}_s^H(n)\mathbf{w}\right]\\ &= \mathbf{w}^H\mathbf{R}_s\mathbf{w}\end{aligned} \tag{26}$$

and the output interference plus noise power at the output is

$$\begin{aligned}\mathbf{P}_{j+\nu} &= E\left[\left|\mathbf{y}_{j+\nu}(n)\right|^2\right]\\ &= E\left[\mathbf{w}^H\mathbf{x}_{j+\nu}(n)\mathbf{x}_{j+\nu}^H(n)\mathbf{w}\right]\\ &= \mathbf{w}^H\mathbf{R}_{j+\nu}\mathbf{w}\end{aligned} \tag{27}$$

The signal to interference plus noise ratio (SINR) is defined as the ratio of signal power to interference plus noise power at the output and can be written as

$$\mathrm{SINR} = \frac{\mathbf{P}_s}{\mathbf{P}_{j+\nu}} = \frac{\mathbf{w}^H\mathbf{R}_s\mathbf{w}}{\mathbf{w}^H\mathbf{R}_{j+\nu}\mathbf{w}} \tag{28}$$

Pseudo code for the proposed APSA-STPAP algorithm based on LCMV is given in Algorithm 1.

Algorithm 1: APSA-STPAP Algorithm Based on LCMV

1: Set the directions and numbers of incoming waves of expected signal and interference signal:
$(\theta_p, f_p, r_p, \eta_p), (\theta_q, f_q, r_q, \eta_q), P, Q$.

2: Set the number of array elements, array element spacing, number of time taps, and number of samples: M, d, K, L .

3: for i=1 to P+Q do

4: Calculate the joint vector of the desired and interference signals:

$\mathbf{s}_{ASTP}(\theta_p, f_p, \gamma_p, \eta_p), \mathbf{s}_{ASTP}(\theta_q, f_q, \gamma_q, \eta_q)$,

5: end for

6: for i=1 to P+Q do

7: for n = 1 to L do

8: Obtain the input signal for the nth sample using (11).

9: end for

10: end for

11: Obtain the covariance matrix using (15).

12: Obtain the constraint matrix using (18).

13: Set the constraint vector using (19).

14: Use (21) to obtain the optimal weight vector.

15: Obtain the array pattern using (22) and (23) which gives the three-dimensional beam pattern.

16: SINR can be obtained from (28).

4 Simulation results

4.1 Array orientation comparison between the APSA-STPAP and DPSA- STPAP algorithms

An eight-element APSA ULA with single wavelength spacing in each direction is employed. Each APSA dipole is followed by a tapped delay line with four taps. The desired signal has a bandwidth of 20.46 MHz and an intermediate frequency of 46.52 MHz. The sampling frequency and number of samples are 62 MHz and 300, respectively. The signal-to-noise ratio (SNR) of the desired signals is − 20 dB, and the interference to noise ratio (INR) of the interference signals is 50 dB. Additive white Gaussian noise (AWGN) with mean 0 and variance 1 is considered. Since the joint polarization-space–time domain has four dimensions, a four-dimensional search is required. To facilitate the discussion, fixed polarization phase angles and intermediate frequencies are used to observe the polarization-space domain pattern, and fixed polarization phase angles and phase differences are used to observe the space–time domain pattern.

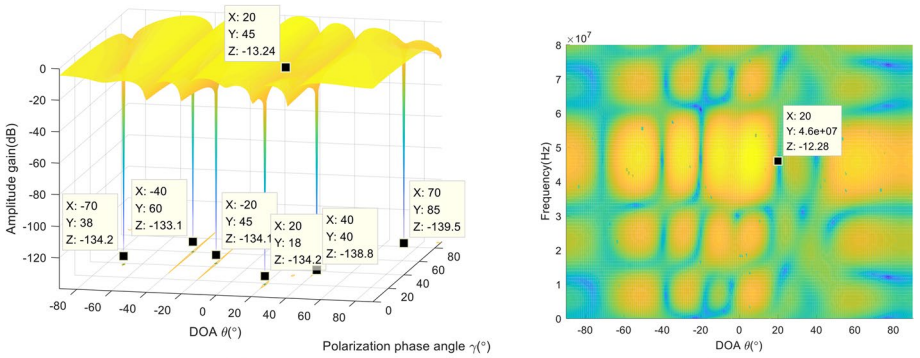

Fig. 5 Three-dimensional beam pattern for the APSA-STPAP algorithm **a** space-polarization domain null pattern and **b** top view of the space–time domain null pattern

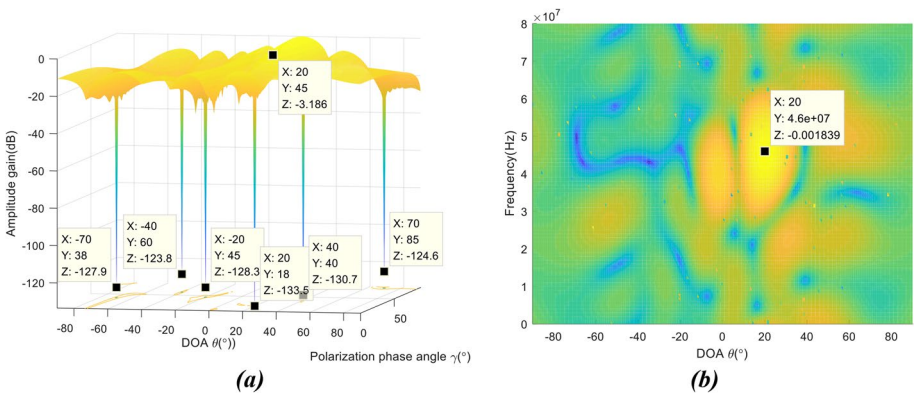

Fig. 6 Three-dimensional beam pattern for the DPSA-STPAP algorithm **a** space-polarization domain null pattern and **b** top view of the space–time domain null pattern

It is assumed that the DOA of the desired signal with RHCP polarization $((\gamma_0, \eta_0) = (45°, -90°))$ is 20° and the DOA of the interference signals are −70°, −40°, −20°, 20°, 40°, and 70°. Further, the time of arrival (TOA) of the desired and interference signals is the same. Two scenarios are considered. In Scenario 1, the intermediate frequency of the interference signals is 46.52 MHz. The parameters are $(\gamma_i, \eta_i) = (38°, -90°), (60°, -90°), (45°, -90°), (18°, -90°), (40°, -90°), (85°, -90°)$, $1 \leq i \leq 6$. In Scenario 2, the interference signals are RHCP with parameters $(\gamma_i, \eta_i) = (45°, -90°)$. The intermediate frequencies are 30 MHz, 35 MHz, 40 MHz, 49 MHz, 55 MHz, and 60 MHz.

The simulation results for the DPSA-STPAP and APSA-STPAP algorithms are given in Figs. 5 and 6, respectively, for Scenario 1, and Figs. 7 and 8 for Scenario 2. In Scenario 1, the directions of the interference and desired signal are the same, so the null can be formed in the polarization domain direction without affecting reception of the desired signal. In Scenario 2, the null can be formed in the frequency dimension direction without affecting the reception of the desired signal. Therefore, the two algorithms have a three-dimensional resolution in the spatial, time, and polarization domains. When the information for two domains is the same, the third domain can be used to distinguish

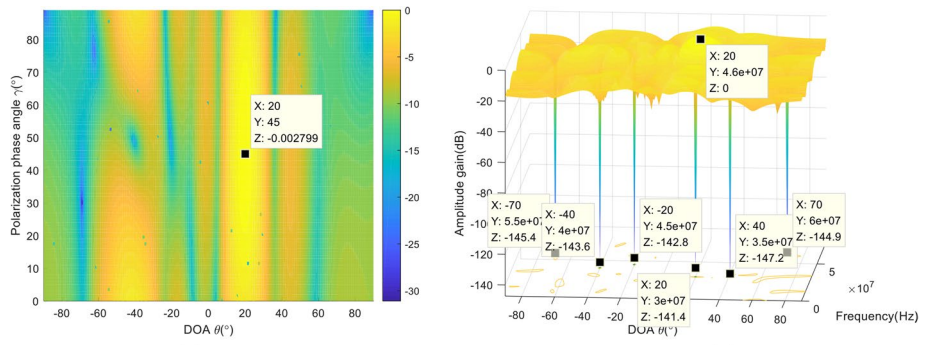

Fig. 7 Three-dimensional beam pattern for the APSA-STPAP algorithm **a** space-polarization domain null pattern and **b** top view of the space–time domain null pattern

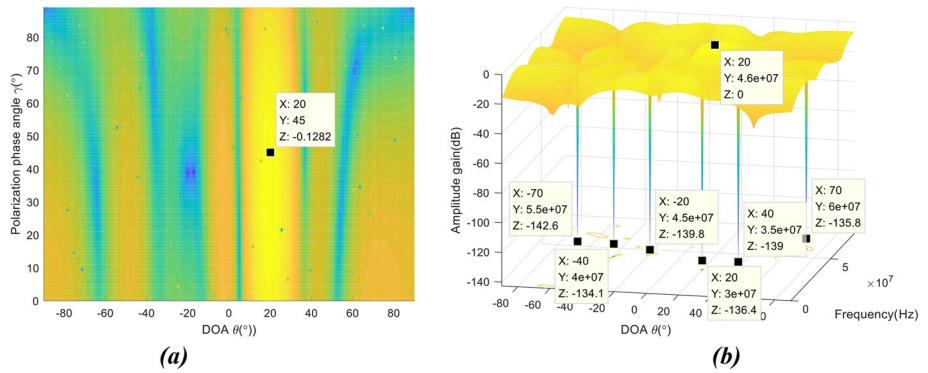

Fig. 8 Three-dimensional beam pattern for the DPSA-STPAP algorithm **a** space-polarization domain null pattern and **b** top view of the space–time domain null pattern

and identify the signals, so the anti-interference performance is improved. These results show that the proposed algorithm can suppress interference without affecting the desired signals when they have the same direction as polarization information is employed for joint polarization-space–time anti-interference. Thus, this is an effective solution for anti-interference when the desired and interference signals have the same DOA.

4.2 Computational complexity

The weight vector for the APSA-STPAP algorithm is given by (21). While a solution can be obtained for multiple input multiple output (MIMO) systems, for computational complexity comparison purposes a single input single output (SISO) system is considered. Determining the optimal weight involves the following four steps.

1. The estimated autocorrelation matrix of the received signals, $\hat{\mathbf{R}}$, is obtained using L signal samples.
2. The inverse matrix $\hat{\mathbf{R}}^{-1}$ is obtained.
3. The joint steering vector $\mathbf{s}_{\mathrm{ASTP}}(\theta, f, \gamma, \eta)$ is calculated.

Table 2 Computational complexity of the DPSA-STPAP algorithm

Operation	Step 1	Step 2	Step 3	Step 4	Total
Real multiplication	$16(MK)^2L$	$32(MK)^3-8(MK)^2$	$16MK$	$16(MK)^2$	$32(MK)^3+16(MK)^2L+8(MK)^2+16MK$
Real division	$8(MK)^2$	$16(MK)^2$	0	0	$24(MK)^2$
Real addition	$16(MK)^2L-8(MK)^2$	$32(MK)^3-8(MK)^2$	$4MK+4M$	$16(MK)^2-4MK$	$32(MK)^3+16(MK)^2L+4M$

Table 3 Computational complexity of the APSA-STPAP algorithm

Operation	Step 1	Step 2	Step 3	Step 4	Total
Real multiplication	$4(MK)^2L$	$4(MK)^3-2(MK)^2$	$8MK$	$4(MK)^2$	$4(MK)^3+4(MK)^2L+2(MK)^2+8MK$
Real division	$2(MK)^2$	$4(MK)^2$	0	0	$6(MK)^2$
Real addition	$4(MK)^2L-2(MK)^2$	$4(MK)^3-2(MK)^2$	$2MK+2M$	$4(MK)^2-2MK$	$4(MK)^34(MK)^2L+2M$

4. The product of $\hat{\mathbf{R}}^{-1}$ and $\mathbf{s}_{\mathrm{ASTP}}(\theta,f,\gamma,\eta)$ is obtained.

Tables 2 and 3 present the computational complexity of the DPSA-STPAP and APSA-STPAP algorithms. These results show that the number of real multiplications, real divisions, and real additions is lower with the APSA-STPAP algorithm. Further, the number of computations is related to the number of samples L, the number of array elements M, and the number of time domain taps K. Fig. 9 presents the total number of computations for the two algorithms versus L, M, and K. These results show the effect of the three variables on the computational complexity. It is clear that the number of operations for the APSA-STPAP algorithm is significantly lower than for the DPSA-STPAP algorithm. This indicates that employing the APSA-STPAP algorithm for space–time-polarization joint anti-interference will reduce the required number of calculations which makes implementation easier.

4.3 Anti-interference performance

The simulation parameters used in Sect. 4.1 are considered here.

4.3.1 Effect of the number of time domain taps

The effect of the number of time domain taps on the SINR is now examined. Figure 10 presents the SINR versus the number of taps with input SNR -10 dB, -20 dB, and -30 dB. The SINR values are the average of 500 Monte Carlo trials.

For low SNRs, i.e., SNR $=-30$ dB and -20 dB, the SINR increases with an increase in the number of taps, and the DPSA-STPAP algorithm is superior to the APSA-STPAP algorithm, but the results are similar with a larger number of taps and SNR $=-20$ dB. With a high signal-to-noise ratio, i.e., SNR $=-10$ dB, the SINR for the two algorithms is similar, but the results for the APSA-STPAP algorithm with more than 3 taps are superior. The main reason is that the zero notch narrows with an increase in the number of taps which reduces the impact on the main lobe. Thus, the signal loss is reduced and the signal-to-interference noise ratio is increased. Further, an increase in the number of taps increases the order of the transverse FIR filter. This

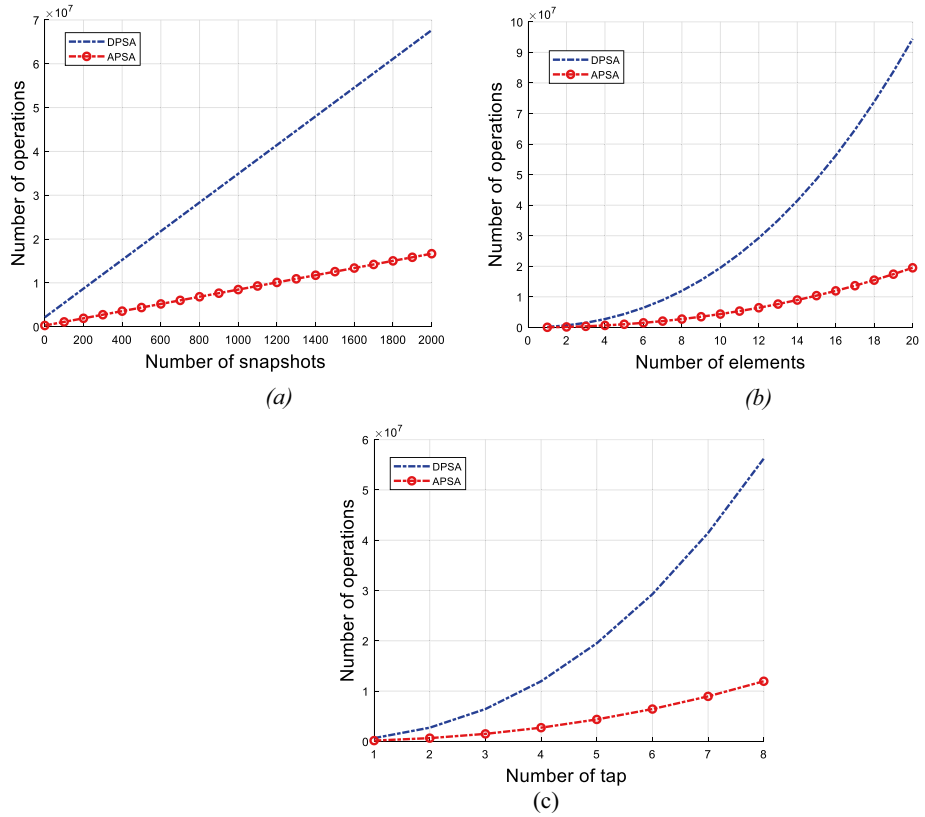

Fig. 9 Computational complexity of the APSA-STPAP and DPSA-STPAP algorithms **a** number of operations versus the number of samples, **b** number of operations versus the number of array elements, and **c** number of operations versus the number of time domain taps

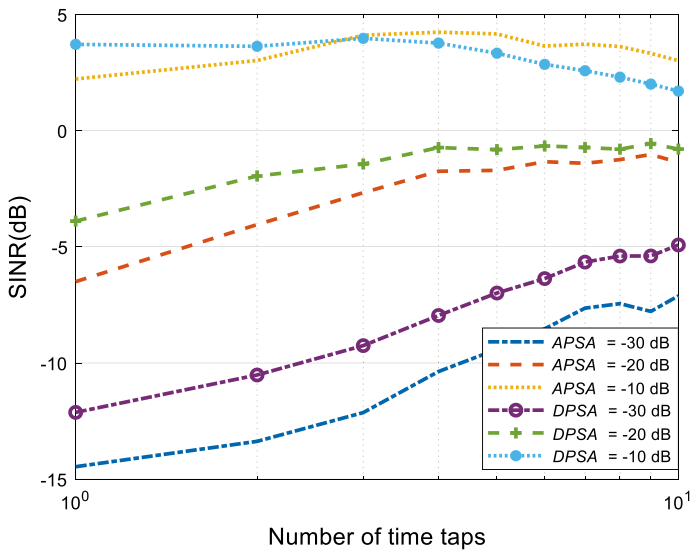

Fig. 10 SINR versus the number of time domain taps

improves the frequency resolution so the interference signal can be suppressed more effectively. However, increasing the number of taps increases the computational complexity. Thus, the maximum number of taps considered here is 10.

4.3.2 Effect of the number of samples

The influence of the number of samples on the output SINR is now considered. Figure 11 presents the SINR versus the number of samples with input SNR -10 dB, -20 dB, and -30 dB. The SINR values are the average of 500 Monte Carlo trials. These results show that the SINR increases with the number of samples and the results for the two algorithms are similar. With a small number of samples, the SINR for the APSA-STPAP algorithm is better than for the DPSA-STPAP algorithm. However, the output SINR of the DPSA-STPAP algorithm is higher with a larger number of samples. The SINR difference decreases as the SNR increases and at SNR $= -10$ dB the results are almost identical for more than 3 samples.

4.3.3 Effect of the input SNR

The effect of the input SINR on the output SINR is now examined. Figure 12 presents the SINR for the two algorithms as the input SNR varies from -40 to -10 dB. The SINR values are the average of 500 Monte Carlo trials. These results show that the SINR for the DPSA-STPAP algorithm is higher than for the APSA-STPAP algorithm. The SINR difference decreases as the SNR increases. The maximum difference in SINR is about 3 dB. Thus, although the dipole and degrees of freedom are half, the anti-interference performance of the APSA-STPAP algorithm is similar to that for the DPSA-STPAP algorithm when SNR ≥ -10 dB.

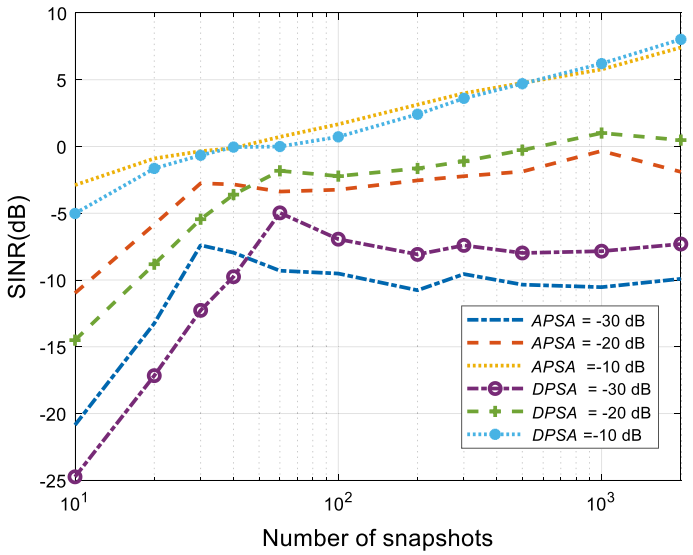

Fig. 11 SINR versus the number of samples

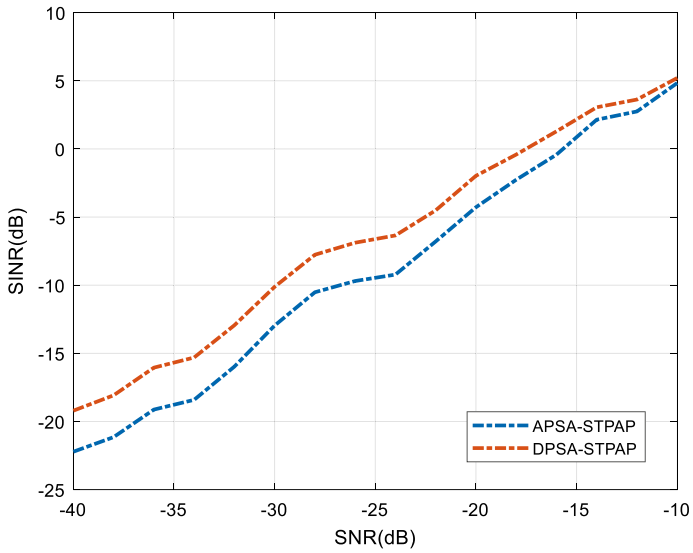

Fig. 12 SINR versus the input SNR

5 Conclusion

In this paper, an APSA-STPAP algorithm based on the LCMV criterion was proposed. This algorithm improves on traditional space–time adaptive algorithms by employing polarization domain information. Simulation results were presented which show that it can effectively suppress interference while enhancing the desired signal. Further, the proposed algorithm has lower computational complexity than the DPSA-STPAP algorithm so it is easier to implement. The results presented indicate that the APSA-STPAP algorithm has anti-interference performance similar to that of the DPSA-STPAP algorithm even though the electric dipole and anti-interference degrees of freedom are reduced by half. There is little difference in anti-interference performance when $\mathrm{SNR} \geq -10$ dB. This paper provides a theoretical basis for the use of polarization-sensitive arrays in multi-dimensional anti-interference.

Abbreviations

APSA: Alternating polarization-sensitive array; DPSA: Dual polarization-sensitive array; LCMV: Linear constraint minimum variance; GNSS: Global navigation satellite system; STAP: Signal time adaptive processing; SPTP: Signal polarization adaptive processing; STPAP: Space–time polarization adaptive processing; FIR: Finite impulse response; ULA: Uniform linear array; TE: Transverse electric; RF: Radio frequency; APSA-STPAP: Alternating polarization-sensitive array space–time polarization adaptive processing; DPSA-STPAP: Dual polarization-sensitive array space–time polarization adaptive processing; SNR: Signal-to-noise ratio; SINR: Signal to interference and noise ratio; DOA: Direction of arrival; HP: Horizontal polarization; VP: Vertical polarization; EP: Elliptical polarization; RHCP: Right-hand circular polarization; LHCP: Left-hand circular polarization.

Acknowledgements

None.

Authors' contributions

TL and SS proposed the APSA-STPAP algorithm. HZ and TAG provided guidance on the analysis and simulations. SS wrote the majority of the manuscript. YD revised the content. All authors read and approved the final manuscript.

Funding

This work was supported by the National Natural Science Foundation of China (Grant No. 61701462), the Marine S&T fund of Shandong Province for Pilot National Laboratory for Marine Science and Technology (Qingdao) (Grant No. 2018SDKJ0210), and the Open Studio for Marine High Frequency Communications, Qingdao National Laboratory for Marine Science and Technology.

Availability of data and materials
Data sharing is not applicable as no datasets were generated or analyzed in this study.

Declarations

Ethics approval and consent to participate
Not applicable.

Consent for publication
Consent is not applicable as this manuscript does not contain personal data in any form (including individual details, images, or video).

Competing interests
The authors declare that this article has no conflict of interest.

Author details
[1]China Open Studio for Marine High Frequency Communications, Pilot National Laboratory for Marine Science and Technology (Qingdao), Institution of Information Science and Engineering, Ocean University of China, Qingdao 266100, China. [2]Department of Electrical and Computer Engineering, University of Victoria, Victoria, BC V8W 2Y2, Canada.

Received: 15 April 2021 Accepted: 3 March 2022
Published online: 21 March 2022

References

1. B. Widrow, P.E. Mantey, L.J. Griffiths et al., Adaptive antenna systems. Proc. IEEE **55**(12), 2143–2159 (1967)
2. I.S. Reed, J.D. Mallett, L.E. Brennan, Rapid convergence rate in adaptive arrays. IEEE Trans. Aerosp. Electron. Syst. **10**(6), 853–863 (1974)
3. L.E. Brennan, L.S. Reed, Theory of adaptive radar. IEEE Trans. Aerosp. Electron. Syst. **9**(2), 237–252 (1973)
4. R. Klemm, Introduction to space–time adaptive processing. Electron. Commun. Eng. J. **11**(1), 5–12 (1999)
5. K. Richard, *Applications of Space–Time Adaptive Processing* (IET Digital Library, 2004)
6. R.L. Fante, J.J. Vaccaro, Wideband cancellation of interference in a GPS receive array. IEEE Trans. Aerosp. Electron. Syst. **36**(2), 549–564 (2000)
7. F.Q. Chen, J.W. Nie, B.Y. Li et al., Distortionless space–time adaptive processor for global navigation satellite system receiver. Electron. Lett. **51**(25), 2138–2139 (2015)
8. R.T. Compton, The tripole antenna: an adaptive array with full polarization flexibility. IEEE Trans. Antennas Propag. **29**(6), 944–952 (1981)
9. R.T. Compton, On the performance of a polarization sensitive adaptive array. IEEE Trans. Antennas Propag. **29**(5), 718–725 (1981)
10. W.C. Cheuk, M. Trinkle, D.A. Gray, Null-steering LMS dual-polarised adaptive antenna arrays for GPS. Positioning **1**(9), 258–267 (2005)
11. J. Wang, G.A. Moeness, Multiple interference cancellation performance for GPS receivers with dual-polarized antenna arrays. EURASIP J. Adv. Signal Process. **2008**, 178 (2008)
12. Y.H. Zhan, S.X. Li, Z. Wang, Algorithm and performance analysis of GPS single dual polarized antenna anti interference. J. Natl. Univ. Defense Technol. **31**(1), 95–98 (2009)
13. F. Fohlmeister, A. Iliopoulos, M. Sgammini et al., Dual polarization beamforming algorithm for multipath mitigation in GNSS. Signal Process. **138**, 86–97 (2017)
14. R.L. Fante, J.J. Vaccaro, Evaluation of adaptive space–time-polarization cancellation of broadband interference. In Proceedings of IEEE Position Location and Navigation Symposium (Palms Springs, 2002), p. 1–3
15. Y.G. Xu, Z.W. Liu, X.F. Gong, *Polarization Sensitive Array Signal Processing*, 1st edn. (Beijing Institute of Technology Press, 2013)
16. X.F. Zhang, H.W. Xu, X.F. Qiu, *Array Signal Processing and MATLAB Implementation*, 1st edn. (Electronics Industry Press, 2015)
17. Z.H. Xu, Z.Y. Xiong, S.P. Xiao, A novel alternate polarization array and its filtering performance. in Proceedings of IEEE CIE International Conference on Radar, Chengdu, China (2011), p. 1890–1892
18. Z.H. Xu, L. Zhang, D.J. Wu et al., Research on filtering performance of alternating polarization array. J. Natl. Univ. Defense Technol. **34**(5), 49–54 (2012)
19. H.J. Dou, D.L. Xiao, S.F. Zhang, Performance analysis of alternating polarization sensitive array projection filtering. J. Beijing Univ. Technol. **2017**, 1 (2017)
20. X. Wang, J. Li, M. Zhang et al., Space–time-polarization adaptive antenna arrays for GNSS receivers. J. Phys. Conf. Ser. **1169**, 1 (2019)
21. H. Wang, Z. Yao, J. Yang et al., A novel beamforming algorithm for GNSS receivers with dual-polarized sensitive arrays in the joint space–time-polarization domain. Sensors **18**, 12 (2018)
22. J. Wu, X.J. Zhu, X.M. He, Z.Y. Gao, Y.B. Fang, Joint estimation of DOA and polarisation for radar signals based on dual-polarised antenna array. IET Microwaves Antennas Propag. **14**(10), 989–998 (2020)
23. X.F. Wang, J.Q. Liu, C. Han et al., Navigation anti-interference method based on polarization sensitive array. Missile Space Carrier Technol. **2017**(2), 50–52 (2017)

24. Y.-H. Chen, J.-C. Juang, D.S. De Lorenzo, et al., Real-time software receiver for GPS controlled reception pattern antenna array processing. in Proceedings of International Technical Meeting of the Satellite Division of the Institute of Navigation, Portland (2010), p. 1932–1941
25. A. Elnashar, Efficient implementation of robust adaptive beamforming based on worst-case performance optimization. IET Signal Proc. **2**(4), 381–393 (2008)

Publisher's Note